Changes in the thickness distribution of Arctic sea ice between 1958–1970 and 1993–1997

Y. Yu, G. A. Maykut, and D. A. Rothrock

Polar Science Center, Applied Physics Laboratory, University of Washington, Seattle, Washington, USA

Received 26 May 2003; revised 28 April 2004; accepted 1 June 2004; published 6 August 2004.

[1] Submarine sonar data collected in the central Arctic Basin during middle and late summer were used to examine differences in the sea ice thickness distribution function $g(h)$ between the periods 1958–1970 and 1993–1997. Cruises during the former period were made in July and August, whereas the 1993–1997 cruises were made in September and October. Seasonal correction was applied to adjust for the differences in thickness. While ice drafts were from only seven submarine cruises and somewhat spatially limited, results indicate that the fractional area covered by open water and first-year ice increased from 0.19 to 0.30 during the time interval. This was balanced by an 11% reduction of level-multiyear and ridged ice. Substantial losses occurred in ice thicker than 2 m, with an increase in the amount of 1–2 m ice. The volume of ice less than 4 m thick remained nearly the same and the total volume decreased about 32%. Losses in the volume of thicker ice increased with increasing thickness. Part of the change in $g(h)$ is likely caused by increased ice area export through Fram Strait in the late 1980s and early 1990s. Because decadal variations in the North Atlantic Oscillation and Arctic Oscillation indices correlate with ice export anomalies, export-induced changes in $g(h)$ probably tend to be cyclical in nature. However, a substantial shift in the peak of $g(h)$ suggests that changes in thermal forcing were also a major factor in the observed thinning. *INDEX TERMS:* 4215 Oceanography: General: Climate and interannual variability (3309); 1863 Hydrology: Snow and ice (1827); 1724 History of Geophysics: Ocean sciences; 9315 Information Related to Geographic Region: Arctic region; *KEYWORDS:* Arctic, sea ice, climate, ice thickness, ice draft distribution

Citation: Yu, Y., G. A. Maykut, and D. A. Rothrock (2004), Changes in the thickness distribution of Arctic sea ice between 1958–1970 and 1993–1997, *J. Geophys. Res.*, *109*, C08004, doi:10.1029/2003JC001982.

1. Introduction

[2] Mounting evidence indicates that significant changes in the state of the Arctic sea ice cover have occurred during the past few decades. Passive microwave observations reveal an increase in the length of the summer melt season over the perennial ice pack [*Smith*, 1998], as well as a gradual decline in sea ice extent since the early 1980s [*Gloersen and Campbell*, 1991; *Parkinson et al.*, 1999; *Walsh and Chapman*, 2001; *Parkinson and Cavalieri*, 2002]. This decline was accompanied by a reduction of multiyear ice coverage in winter and a corresponding increase in the amount of first-year ice coverage [*Johannessen et al.*, 1999]. Ice draft measurements made during submarine cruises show that mean ice thickness has also decreased dramatically [*Rothrock et al.*, 1999]. In that study, late summer data acquired during the Scientific Ice Expeditions (SCICEX) program in the 1990s were compared with similar data from earlier cruises at 29 locations within the central Arctic Basin (Figure 1a). Results showed that mean ice draft over deep water portions of the Arctic Ocean was about 1.3 m less in the 1990s than 30 to 40 years earlier (Figure 1b). This result agrees with the analysis of British submarine data collected in the Eurasian Basin [*Wadhams and Davis*, 2000]. Spring cruise data collected across the Canada Basin to the North Pole likewise showed a decrease of about 1.5 m in mean ice draft between the mid-1980s and the early 1990s [*Tucker et al.*, 2001].

[3] Coincident with the changes in sea ice cover have been substantial changes in the atmosphere and ocean across the Arctic Basin. Studies show that average sea level pressure decreased in the early 1990s [*Walsh et al.*, 1996], while surface air temperatures increased, particularly in the eastern Arctic during winter and spring [*Martin et al.*, 1997]. The lower sea level pressure has been related to decadal shifts in the wind-driven circulation of the Arctic Ocean [*Proshutinsky and Johnson*, 1997]. This is supported by ship-based field observations that show warmer Atlantic water in the Eurasian Basin [*Quadfasel*, 1991], a retreat of the cold arctic halocline within the same region [*Steele and Boyd*, 1998], and increased surface salinity in the Makarov Basin under the greater influence of Atlantic water [*Carmack et al.*, 1995; *Morison et al.*, 1998].

[4] Long-term changes in the arctic environment will inevitably affect the state of the sea ice cover through both dynamic and thermodynamic processes. Dynamics produce changes in sea ice concentration and in the

0148-0227/04/2003JC001982$09.00

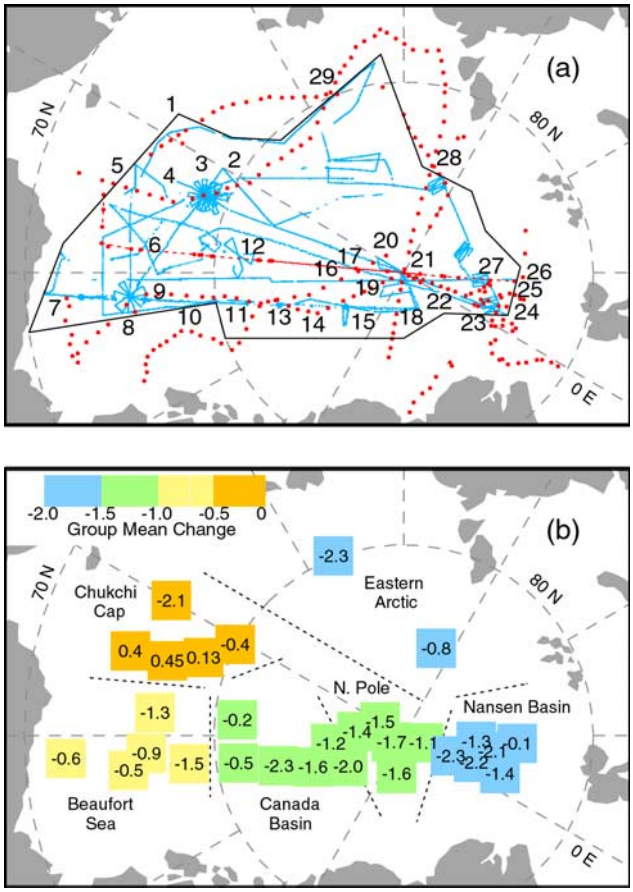

Figure 1. (a) Submarine cruise tracks used in this analysis. Tracks from the early cruises (1958–1976) are indicated by dotted red lines, and those from the 1990s are indicated by solid blue lines. The numbers indicate locations where comparisons were made. The area from which SCICEX data could be released is the interior of the solid black polygon, the so-called "SCICEX Box." (b) Changes in mean draft from the early period to the 1990s. The change at each numbered crossing is shown numerically. The crossings within each regional group are given the same shading equivalent to their group means. From *Rothrock et al.* [1999].

amount of ridged ice through variations in ice deformation and transport [*Maslanik and Dunn*, 1997]. Thermodynamic processes dominate the annual thickness cycle and strive to maintain an equilibrium in ice thickness [*Maykut and Untersteiner*, 1971]. Regional ice volume can be modified by long-term changes in thermal forcing, or by changes in the distribution of ice thickness related to dynamic processes. While either dynamics or thermodynamics can alter the mean thickness of the ice pack, these processes normally interact, making their effects on the ice cover difficult to separate. Ice divergence, for example, generates open water and reduces average ice thickness; at the same time, thermodynamics act to mitigate these changes through rapid ice production in the newly opened leads and areas of thin ice. In the case of ice thinning due to climatic warming, the magnitude of the observed decrease in average ice thickness could have been enhanced by a more divergent ice motion field, or reduced by greater convergence. This interplay between ice dynamics and thermodynamics has been demonstrated in a modeling study by *Zhang et al.* [2000] showing that interannual variability in sea ice concentration and thickness is driven by both anomalous ice advection and summer melting.

[5] Although previous studies have focused on changes in average ice thickness, it is clear that the reason for such changes can be difficult to interpret from this information alone. A decline in mean ice thickness could be simply the result of an increase in thin ice, or it might reflect a decrease in the amount of thicker ridged ice, or both. Here we revisit the data used by *Rothrock et al.* [1999], looking this time at changes as a function of ice thickness to see whether there are clues as to the cause of the observed differences.

2. Approach

[6] The large-scale response of sea ice to environmental changes depends primarily on its aggregate properties characterized by the ice thickness distribution $g(h)$, a probability density function describing the relative area covered by different thicknesses of ice within a particular region. This function is defined as

$$\int_{h_1}^{h_2} g(h)\,dh = A(h_1, h_2)/R, \tag{1}$$

where R denotes the total area of some region R and $A(h_1, h_2)$ is the area within R covered by ice with thickness h in the range $h_1 \le h \le h_2$ [*Thorndike et al.*, 1975]. Changes in $g(h)$ alter not only the mean ice thickness, but also the large-scale mechanical properties and regional heat and mass balance of the ice cover. Information about $g(h)$ is thus of fundamental interest in a wide variety of scientific and engineering applications. The most practical way to estimate $g(h)$ at present is to use submarine sonar records taken from cruises, which typically yield ice draft data with a horizontal resolution of about one meter over distances of thousands of kilometers. Ice draft d is the vertical distance from sea level to the bottom of the ice and accounts for about 90% of the ice thickness. It can be converted to thickness by assuming that the ice is, on average, in hydrostatic equilibrium with an average density of 900 kg m^{-3}, meaning that $h \approx 1.11d$. Converting to h is often useful for comparison with model results and for computing thickness dependent quantities such as ice volume.

[7] Here we focus on the distribution of ice draft and thickness in the central Arctic using data collected during the same submarine cruises described by *Rothrock et al.* [1999]. Ice draft data derived from three SCICEX cruises in the mid-1990s were first used to examine year-to-year differences in six different regions. Interannual variability is found to be significant. To facilitate comparison with earlier data taken 1958–1970, the SCICEX data were reanalyzed to obtain distributions with a draft bin of 1 m. Results from the SCICEX cruises were then separated into four regions and averaged over the 3-year period. Comparison with similar averages from the 1958–1970

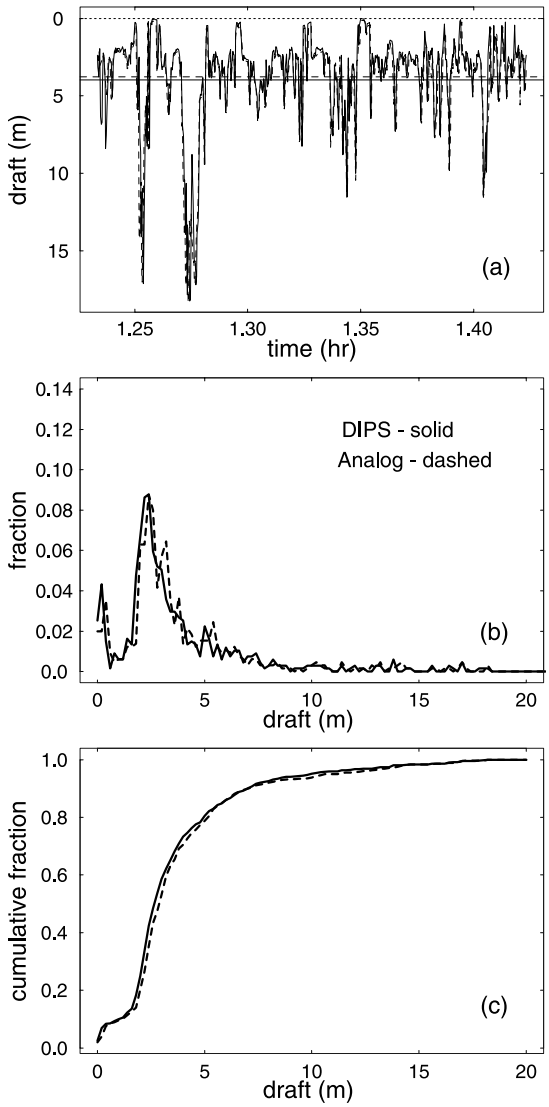

Figure 2. Ice draft comparison between analog chart and Digital Ice Profiling System for (a) profiles, (b) area fraction, and (c) cumulative distribution. The data were recorded along a 5-km SCICEX transect on 9 September 1997.

cruises in these four regions show major changes in $g(h)$ between these two periods. Possible reasons for these changes are discussed.

3. Ice Draft Observations

[8] Data used in the analysis were obtained by seven U.S. submarine cruises that took place during middle to late summer. The four earlier cruises were made between 1958 and 1970, specifically, August 1958 (USS *Nautilus*), August 1960 (USS *Seadragon*), July–August 1962 (USS *Seadragon*), and August 1970 (USS *Queenfish*). Cruise tracks during this period are indicated by the red lines in Figure 1a. Data for the 1990s were taken from three late summer SCICEX cruises: September 1993 (USS *Pargo*), September–October 1996 (USS *Pogy*), and September 1997 (USS *Archerfish*), indicated by solid blue lines in Figure 1a. While SCICEX data provide more extensive coverage of the central Arctic than the earlier data, there are areas of considerable overlap between the two periods, providing an opportunity to quantify changes in $g(h)$ in several regions over a roughly 30-year time interval.

[9] Ice draft data were typically collected from a depth of 100 m using a narrow-beam sonar that sampled a footprint approximately 5 m across at the bottom of the ice. Sonar distances were calibrated frequently using the depth gauge of the submarine and periodic segments of open water. For the SCICEX cruises ice drafts were recorded with the Digital Ice Profiling System (DIPS), which sampled ice draft six times per second. This corresponds to one measurement every meter at a speed of 12 knots. However, because boat speed was not constant throughout the transects, ice draft data were interpolated to produce horizontal profiles with a uniform sampling interval of about 1 m. These interpolated profiles were then used to derive the distributions reported below.

[10] Ice drafts from earlier cruises, however, were digitized manually from analog recording charts using a curve follower and a digitizer table. First acoustic returns were recorded at about 1-s intervals along the envelope of the ice draft profile, then interpolated to ensure sampling intervals of about 1 m [*Bourke and McLaren*, 1992]. Before comparing these measurements with the SCICEX data, the agreement between values of d obtained with the digitized analog charts and with the DIPS was estimated. This was possible because the SCICEX cruises recorded data on both DIPS and charts simultaneously. With newly developed software, a number of 10-min long ice draft profiles (corresponding to a distance of about 5 km on average) from the SCICEX '97 cruise were digitized from the analog charts by taking the first acoustic returns at a sample rate of one data point per second (M. Wensnahan, 2001, personal communication). This computer-automated procedure essentially mimicked the work of the curve followers used in earlier years. To simulate this procedure with the digital data, DIPS records were resampled by taking the maximum draft per six pings (i.e., per second), assuming these values would correspond to the first returns recorded in the analog data. This resampling procedure was used in the following analysis whenever data from SCICEX and the earlier cruises were compared. Tests with more densely sampled DIPS data showed that this resampling procedure did not significantly change the shape of the draft distribution.

[11] Comparison of profiles produced by the two different recording systems showed that while the mean draft from DIPS averaged about 0.2 m thinner than that of the analog charts, both systems recorded all leads and ridges along the transect and tracked each other very closely (Figure 2a). A comparison of area fraction (Figure 2b) and cumulative distribution (Figure 2c) also produced very good agreement. Similar agreement was obtained with other transect comparisons. Note that in Figure 2 the bias occurs randomly within the distribution, making it difficult to compensate for this mean bias. For reasons discussed in

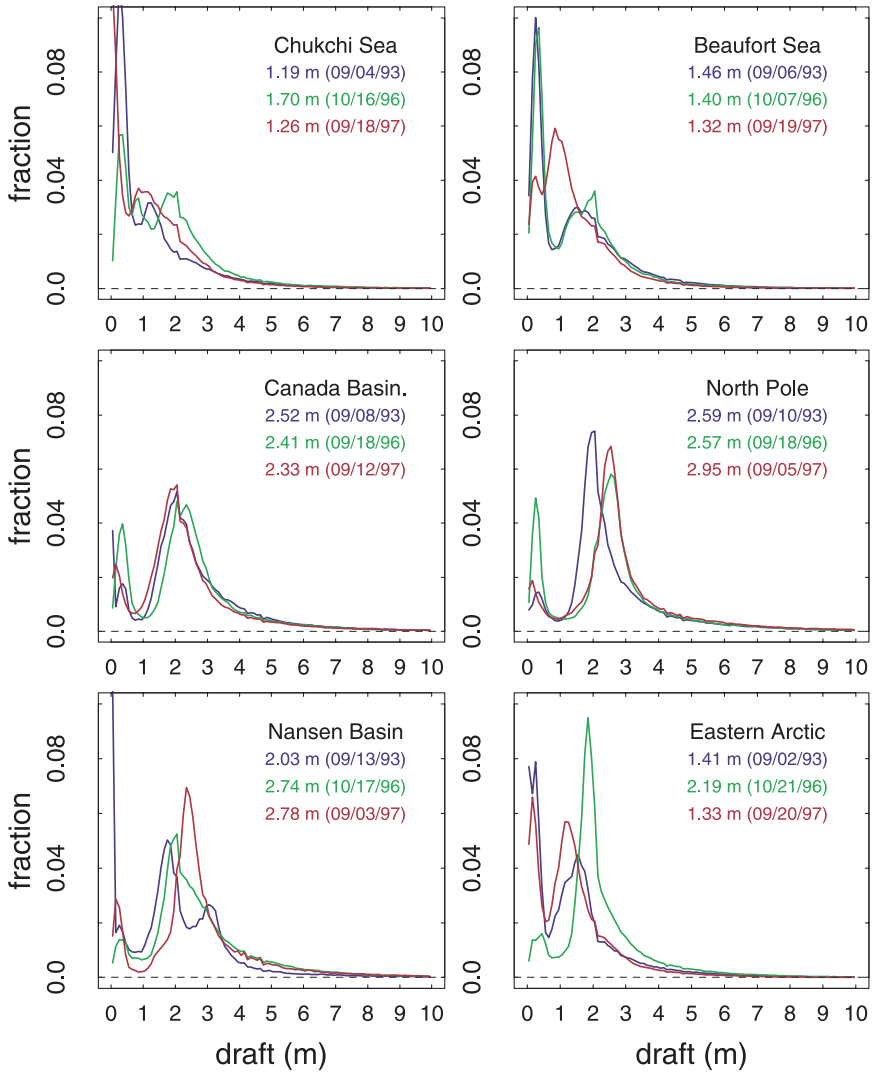

Figure 3. Regional ice draft distributions from the three SCICEX cruises in 1993, 1996, and 1997. The draft bin is 10 cm. Locations of the six areas are shown in Figure 1b. Average draft and date of each transect are also shown.

section 5, we did not apply any bias correction to the distributions from either period.

4. SCICEX Ice Thickness Distributions

[12] Before examining longer-term changes we first looked at spatial and interannual variations in draft observed during SCICEX cruises in 1993, 1996, and 1997. Ice draft distributions were computed from DIPS data using 10-cm bins in each of the six regions shown in Figure 1b. Rather than being limited to just those crossings defined by *Rothrock et al.* [1999], the results here include all ice draft measurements made within each region. Thus our statistics generally cover a broader area and include more data from each region. It should be noted, however, that uncertainties in some of the DIPS data caused us to discard occasional points that may have been open water. As a result, open water fractions reported below may significantly underestimate the true values.

[13] Figure 3 shows regional and temporal differences observed during the 1990s cruises. While there are significant differences among regions and years, all the curves have a local minimum near $d = 1$ m. This minimum appears to mark the boundary between first-year and multiyear ice. Ice to the left of this minimum is mostly young and recently rafted ice, while ice immediately to the right is mostly second-year ice that has survived the proceeding summer melt season. In areas with large amounts of seasonal ice (e.g., the Chukchi Cap and Beaufort Sea), the fall distribution is dominated by the young first-year ice. In areas of perennial ice (e.g., the Canada Basin and North Pole), the second-year ice is replaced by older multiyear ice and reaches a maximum in the distribution where 2.0 m $\leq h \leq$ 2.5 m (i.e., 2.2 m $\leq h \leq$ 2.8 m). The thickness distribution theory of *Thorndike et al.* [1975] predicts that with sufficient time, this maximum should occur near the thermodynamic equilibrium thickness H_e defined by *Maykut and Untersteiner* [1971], while ice to the right of H_e should largely be composed of ridged ice. This picture is supported

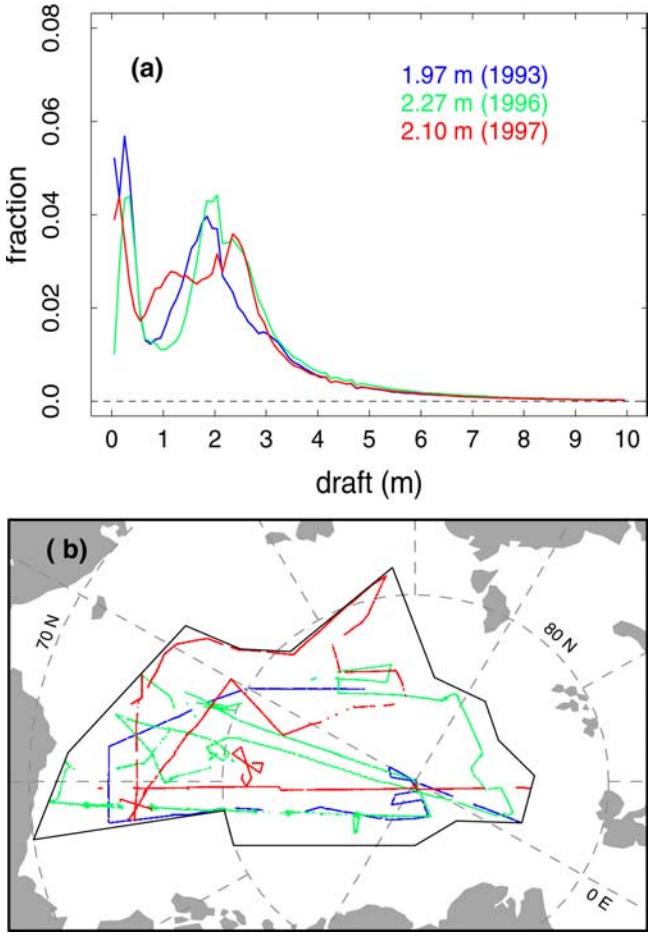

Figure 4. (a) SCICEX ice draft distributions averaged over the entire cruise track for each year. (b) Locations with usable ice draft data in 1993 (blue), 1996 (green), and 1997 (red).

by the SCICEX transect records, which showed almost no smooth ice above 4 m draft.

[14] The peak of $g(h)$ in the Nansen Basin and eastern Arctic, which generally lie within the Transpolar Drift Stream, occurred at somewhat smaller drafts than in the central Arctic. This could be due to regional differences in climate, to large contributions of thin ice from the Laptev Sea, to the presence of younger ice that did not have sufficient time to approach equilibrium, or to some combination of the three. Year-to-year variability in the location of the multiyear maximum was significant. Between 1993 and 1996 all the peaks shifted toward thicker ice; the changes were most prominent in the eastern Arctic and around the North Pole. Changes from 1996 to 1997 were much less consistent. The peaks generally moved toward thinner ice in the eastern Arctic, the Chukchi Cap, the Beaufort Sea, and the Canada Basin. However, the change was minimal around the North Pole, and the peak even moved toward thicker ice in the Nansen Basin. These differences (Figure 3) cannot be explained by differences in cruise dates, i.e., by differences in the amount of new ice produced between early September and early October. The most dramatic change was in the Beaufort Sea where multiyear draft appears to have decreased by about 1 m. This change would require a freshening of the upper ocean, which was observed in fall 1997 [*McPhee et al.*, 1998; *Macdonald et al.*, 2002].

[15] Variations in average draft during the SCICEX cruises were much larger in the Transpolar Drift Stream (i.e., the Nansen Basin and the eastern Arctic) than in the central Arctic, about 75 cm versus 15–35 cm. This is unlikely to reflect year-to-year changes in thermal forcing but rather differences in the relative amounts of multiyear and first-year ice in the Drift Stream. In the eastern Arctic, for example, there was a major increase in the amount of multiyear ice in 1996, which produced a strong peak at about 1.8 m. A similar peak was found in the Nansen Basin the following year, located this time at about 2.2 m. It appears that there was a temporary change in drift patterns in 1996 that advected thicker ice from the western Arctic into the Drift Stream. This ice then thickened by about 40 cm during the following year as it moved toward Fram Strait.

[16] Figure 4a shows ice draft distributions for each of the three SCICEX cruises, averaged over all six regions from the track segments in Figure 4b. The maximum year-to-year variation in average draft within the basin is 30 cm, due primarily to changes in the distribution of 1–3 m ice. The year 1997 appears to have been unusual, with a substantial decrease in the amount of 1.5–2.2 m ice and an increase in the amount of 0.5–1.5 m ice occurring in the Chukchi Cap, Beaufort Sea, and eastern Arctic.

[17] Ice conditions in the Canada Basin varied interannually. The distribution of thinner ice in peripheral regions like the Chukchi Cap and the Beaufort Sea is sensitive to the location of the summer ice edge so substantial year-to-year variations are to be expected, particularly during the fall. The ice cover in the eastern Arctic, the Nansen Basin, and to some extent, the North Pole sector is made up of a constantly changing mixture of thicker ice from the western Arctic and younger ice from the eastern marginal seas, leading to fairly large interannual variability in these sectors as well. While differences in the individual cruise tracks could be a factor, Figure 4a shows that there is a strong interannual variability in the thickness, presumably reflecting changes in drift patterns and thermal forcing.

5. Comparisons Between 1958–1970 and 1993–1997

[18] Two sets of analyzed ice draft distributions from the 1958–1970 period were available for the comparisons. The first were estimates from the 1960 and 1962 cruises made by *Tucker and Hibler* [1986]. These data, also published by *LeSchack* [1980] and used by *Rothrock et al.* [1999], were grouped into 1-m bins up to a thickness of 12 m where the cumulative fraction reached at least 98–99% of the total area. The second set was computed by *McLaren* [1989] from the 1958 and 1970 cruises. His data were grouped into irregularly spaced thickness bins, and any ice thicker than 4 m was assigned to a single, deformed category. By constructing cumulative distributions we were able to interpolate data from these irregular bins into regular 1-m bins so that they could be combined with the 1960 and 1962 data.

[19] To compare the earlier data with the SCICEX observations, we regrouped the SCICEX data into similar 1-m

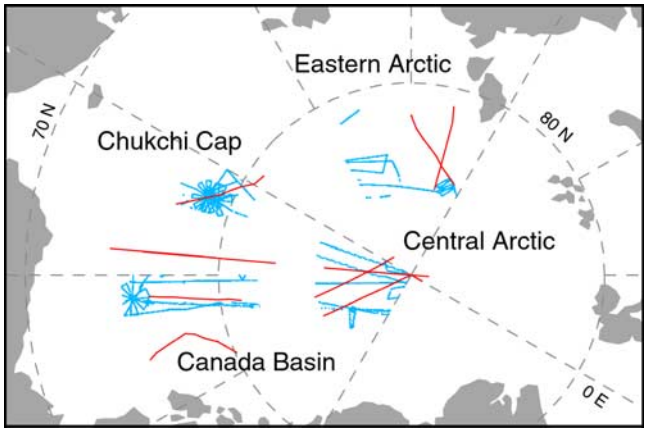

Figure 5. Submarine cruise tracks used to compute thickness distributions in four regions during 1958–1970 (red) and 1993–1997 (blue).

bins. Although coarse, this bin size does allow rough identification of the amounts of major ice types. For convenience, we define first-year as thickness 0–1 m, level-multiyear 1–3 m, and ridged ice >3 m. Figure 5 shows the track segments used in the comparisons. Although these tracks do not overlap entirely, there are four general regions where substantial amounts of draft data were collected during both time periods: the Chukchi Cap, the Canada Basin, the central Arctic, and the eastern Arctic. There are at least 500 km of data available from each of these regions during each period.

[20] Because of differences in season and unresolved issues with some of the DIPS open water data, we did not attempt to estimate changes in open water fraction between the two periods. Comparisons of first-year ice were also complicated because the earlier data were taken during the summer melt season when a considerable amount of open water was often present (e.g., over 20% in the Chukchi Cap sector), while the SCICEX data were taken during the following month after young ice had formed in most of these open water areas. To compare the two data sets it was therefore necessary to estimate how much of the open water from summer would be covered by young ice in September. Using ice strain data from the Beaufort Sea, *Maykut* [1982] calculated that the average amount of open water in September was about one third the average amount in August. On the basis of these results, a seasonal correction was applied by simply transferring two thirds of the open water observed in the 1958–1970 data into the 0–1 m category. Even though this correction is crude, the resulting values (Figure 6) appear to be consistent with those from SCICEX.

[21] It was noted in section 3 that mean drafts calculated from the analog data had a positive bias of 20 cm or more when compared to the digital data. While it would be straightforward to compensate for this bias, we did not think it was necessary in this case. Thicker ice measured in the 1958–1970 cruises would have continued to thin throughout the remainder of the summer, with some bottom ablation occurring even during September [*Maykut and McPhee*, 1995; *Perovich et al.*, 2003]. Total thinning during this period could have easily reached 20–30 cm, roughly balancing the measurement bias. For this reason, we did not apply any corrections when $h > 1$ m.

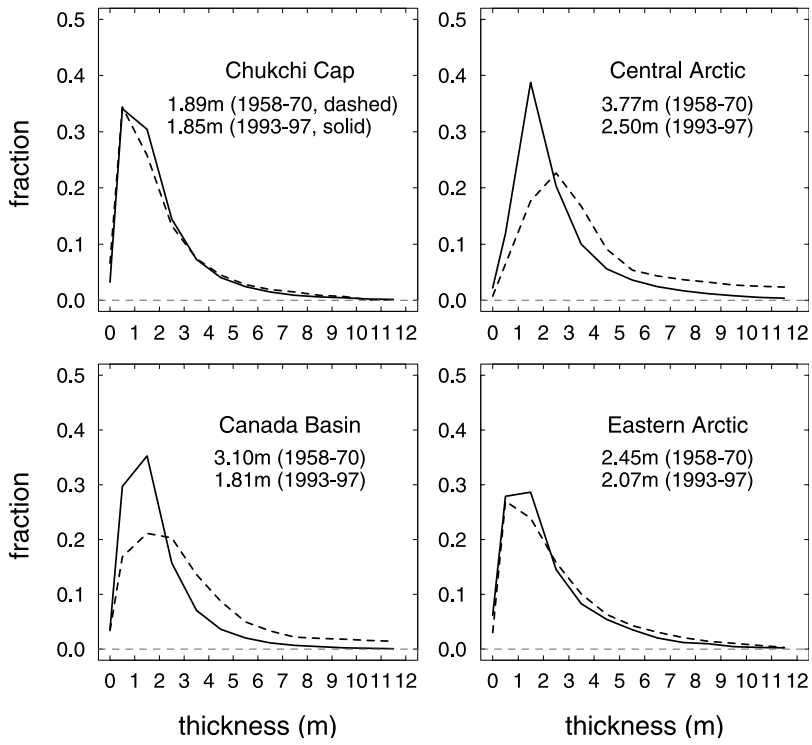

Figure 6. Comparison of ice thickness distributions for the four regions defined in Figure 5. The numbers under each region name are averaged ice thickness for each time period.

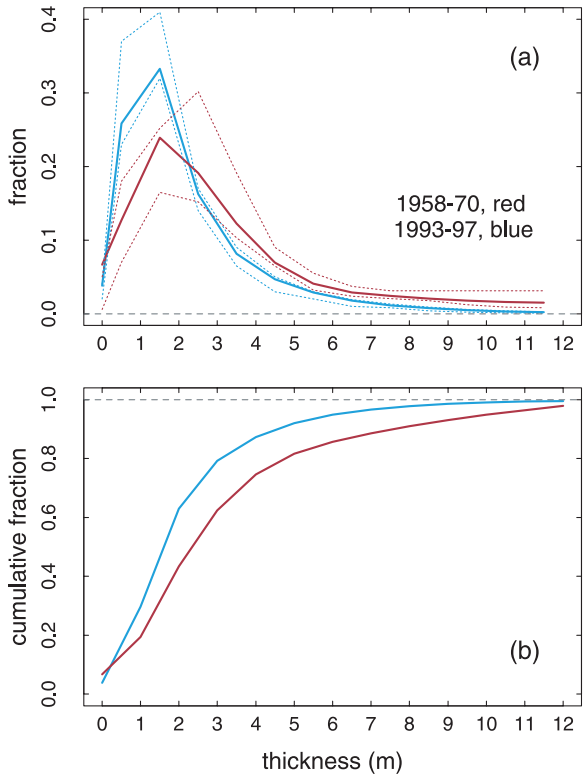

Figure 7. (a) Ice thickness distributions averaged over all four regions during each time period along with averaged maximum and minimum values. (b) Corresponding cumulative thickness distributions.

5.1. Differences in Ice Thickness Distributions

[22] Ice draft data in each of the four regions were averaged within each time period and then converted to ice thickness using the relationship $h = 1.11d$. Resulting $g(h)$ distributions for 1958–1970 and 1993–1997 are plotted in Figure 6. Differences between the two periods clearly varied by region. Average thickness in the Chukchi Cap region, for example, remained essentially unchanged despite a small increase in 1–3 m ice and a corresponding decrease in ice thicker than 3 m. A similar pattern existed in the eastern Arctic, but there was a greater loss of thicker ice and the average h decreased by over 35 cm. It was in the center of the basin, however, where the largest changes occurred. Average thickness in the Canada Basin and central Arctic sectors decreased by about 1.3 m, due primarily to consistent losses in all categories of ice thicker than 3 m. While there were only small losses from the 2–3 m category, there were large increases in ice thinner than 2 m.

[23] This pattern is evident in Figure 7a, which shows $g(h)$ values obtained by averaging all the ice draft data taken during each of the two time periods. The maximum and minimum values averaged for each period are also plotted to represent the "interperiod" variability. The differences in the distributions between the early and the SCICEX cruises are clearly evident. Shown in Figure 7b is the corresponding cumulative distribution $G(h)$, which describes the fractional area occupied by ice with thickness less than or equal to h. Overall, the fractional area of first-year ice ($h < 1$ m) roughly doubled, from 0.13 in 1958–1970 to 0.26 in 1993–1997; this was accompanied by a corresponding increase of 38% in the amount of ice between 1 and 2 m. The area covered by all other ice categories decreased. There was a 16% loss in the area of 2–3 m ice and a 42% loss for ice thicker than 3 m, from a concentration of 0.36 to 0.21. The concentration of ridged ice ($h > 3$ m) in these regions decreased from 0.79 to 0.70. This 11% reduction is consistent with an analysis of satellite-derived microwave data that indicates a 14% loss of multiyear ice between 1979 and 1998 [*Johannessen et al.*, 1999]. The Q-Q plot in Figure 8 shows the large departure in the 1990s from that in the earlier years, with the largest deviations appearing at the thicker end of the distribution and the tail skewed toward thinner ice.

5.2. Differences in Ice Volume

[24] The probability density function describing ice volume is $V(h) = hg(h)$. This function describes the fraction of total volume supplied by ice with thickness h. It is dimensionless and integrates to the mean thickness

$$\overline{h} = \int_0^\infty V(h)\, dh. \tag{2}$$

Figure 9 shows ice volume as a function of h in the four regions during each time period. As with ice area (Figure 6), volume changes were small in the Chukchi Cap and eastern Arctic sectors. Volume losses were much larger in the central Arctic and Canada Basin where there was a strong shift in the peak of the distribution toward thinner ice. In the panel for the central Arctic, the increased fraction at the thicker end of the distribution is introduced artificially because of the linear interpolation for ice thicker than 4 m from the 1958 and 1970 cruises. This will undoubtedly cause additional uncertainty at the tails of the distribution. However, the interpolation produced slightly less thick ice

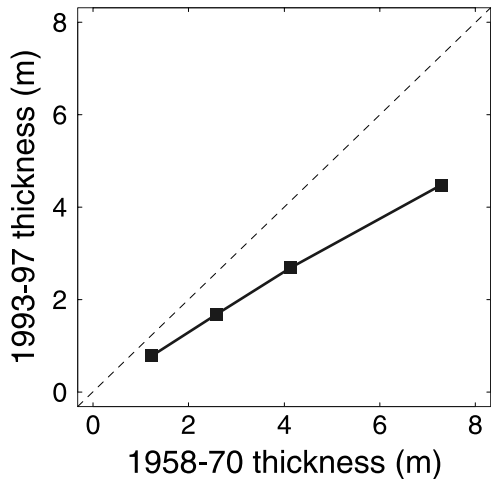

Figure 8. Q-Q plot comparing the ice thickness distribution in 1958–1970 (x axis) to that in 1993–1997 (y axis). Each square (from left to right) represents thickness distributions at 25%, 50%, 75%, and 90%. The dashed line indicates a 1:1 ratio where there would be complete agreement between the two distributions.

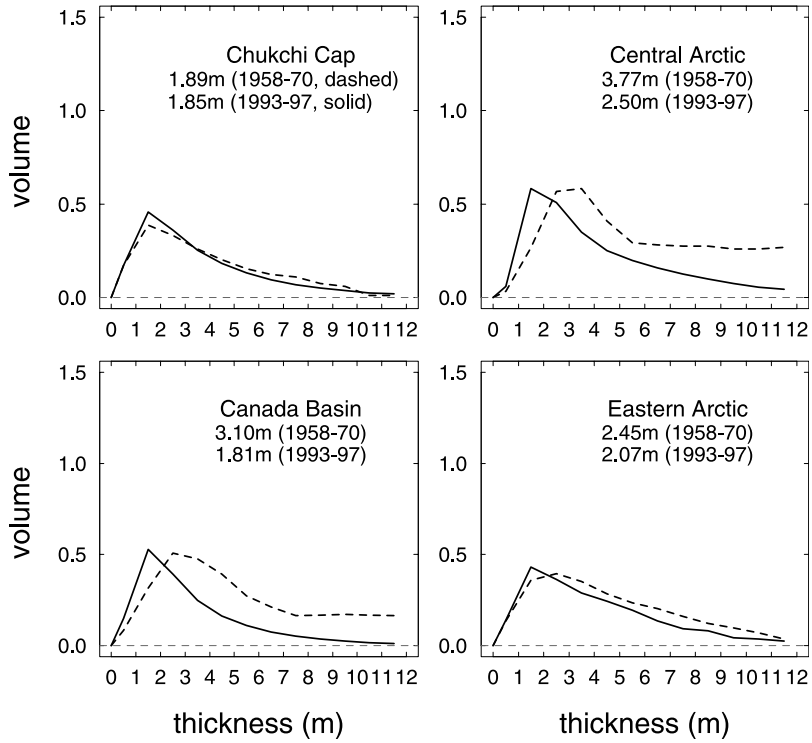

Figure 9. Ice volume as a function of ice thickness for the four regions defined in Figure 5. For comparison the mean ice thicknesses, which represent the total volumes, are shown again for each time period.

when compared with those from the 1960 and 1962 cruises. Therefore we believe that the uncertainty introduced by the interpolation would not change our overall conclusion discussed in the following sections.

[25] For the whole basin there was a net volume loss from all categories of ice thicker than 2 m (Figure 10). Overall, the volume of 0–1 m ice was about twice as large during the 1990s as during 1958–1970, while the volume of 1–2 m ice increased by 39%. On the basis of the limited data available the total net loss of ice volume between 1958–1970 and 1993–1997 was over 30%. It is striking that ridged and multiyear ice account for nearly all the change in ice volume. The volume of ice thinner than 4 m remained essentially unchanged (Figure 10b). It is evident from Figure 10a that volume reductions increased with increasing thickness, ranging from about 16% at 3 m to 86% at 12 m. This observed pattern suggests a long-term depletion of ridged ice through either increased bottom melting and/or decreased ridging.

6. Discussion

[26] According to *Thorndike et al.* [1975], changes in the ice thickness distribution are governed by

$$\frac{\partial g}{\partial t} = -\nabla g \cdot \mathbf{u} - g\nabla \cdot \mathbf{u} - \frac{\partial}{\partial h}(fg) + \psi, \qquad (3)$$

where the terms on the right-hand side of the equation describe the processes of ice advection, divergence, thermodynamic ice growth and melting, and mechanical formation of pressure ridges and open leads. In the

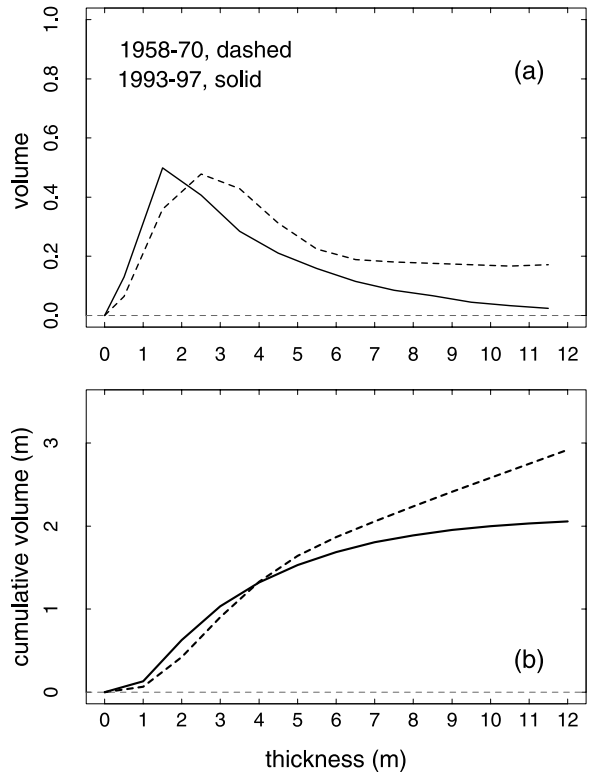

Figure 10. (a) Ice volume as a function of ice thickness averaged over all four regions during each time period. (b) Corresponding cumulative volume as a function of ice thickness.

following sections, we discuss these processes and their possible role in the observed changes in $g(h)$.

6.1. Changes in Ice Advection Patterns

[27] Advection constantly moves ice from one region to another in the Arctic. A net transport of ice out of a particular region would reduce the average ice thickness in that region, even if there were no change in ice growth or ablation. It is reasonable, therefore, to examine whether advection may have played some role in altering $g(h)$. Because there was no ice buildup in any of the sampled regions, any contribution of advection to the observed thinning must have involved removal of ice from the sampling box (Figure 1a), as opposed to a redistribution within the box.

[28] It has, in fact, been suggested that the reduced ice volume observed during the SCICEX cruises was due primarily to changes in ice drift patterns rather than to changes in thermal forcing. While few direct measurements are available from the earlier period, numerical simulations do suggest a shift in ice motion fields, from a strongly anticyclonic pattern before 1990 to a weaker one in the 1990s [*Proshutinsky and Johnson*, 1997]. Recent model calculations have investigated this circulation change and its impact on ice volume between the 1950s and the 1990s [e.g., *Polyakov and Johnson*, 2000; *Holloway and Sou*, 2002]. Though differing in magnitude, both studies report a decline in mean ice thickness similar to that observed by submarines in the sampled regions. However, both studies also predict an ice "pileup" along the Arctic Ocean periphery, particularly in the southern Beaufort Sea and Canadian Archipelago. If this stored ice exists, the reduction in ice volume for the entire Arctic Basin would be much smaller than indicated by the submarine data.

[29] Because ice advection patterns are largely driven by winds, predicted changes in ice volume are especially sensitive to the wind fields and wind stresses used to force the models. A coupled ice-ocean model simulation (J. Zhang, personal communication, 2003) using daily rather than monthly wind forcing predicts an ice build up in the nearshore region of only about 10 cm between 1958–1970 and 1993–1997, roughly 1 order of magnitude less than would be required to explain the amount of ice lost from the central basin. Likewise, late September ice charts from the National Ice Center in the 1990s (available at http://www.natice.noaa.gov/products/arctic) show open water and low ice concentrations in parts of the southern Beaufort Sea predicted to have very thick ice. While buoy motions during the 1990s do show a smaller, weaker Beaufort Gyre and somewhat greater transport of ice toward the Canadian Archipelago, there does not appear to be any independent evidence of a massive buildup of ice outside the SCICEX box that could compensate for the loss of ice volume observed in the central basin. It is much more likely that the apparent volume loss is the result of increased ice export through Fram Strait and/or changes in melting/freezing due to regional warming.

6.2. Changes in Ice Export

[30] The primary outlet for ice export from the Arctic Basin is Fram Strait. Observations from upward looking sonars moored in Fram Strait during the 1990s show a pronounced interannual variability in ice volume flux [*Vinje et al.*, 1998]. Annual values ranged from a minimum of 2050 $km^3\ yr^{-1}$ in 1990–1991 to a maximum of 4700 $km^3\ yr^{-1}$ in 1994–1995. The data indicate that the variability in volume flux during this period was largely due to changes in area flux, rather than to any changes in mean ice thickness or thickness distribution.

[31] An 18-year time series of ice export through Fram Strait between 1978 and 1996 has been derived from satellite observations using combined data sets from SMMR (scanning multichannel microwave radiometer) and SSM/I (Special Sensor Microwave Imager) by *Kwok and Rothrock* [1999]. They report that the ice area flux through Fram Strait averaged about 670,000 $km^2\ yr^{-1}$ during this period and estimate an average volume flux of 1745 $km^3\ yr^{-1}$ between 1990 and 1995. Despite large daily, monthly, and annual variations, they note that there was a gradual increase of about 9900 $km^2\ yr^{-1}$ in the area flux throughout the 1978–1995 period, an upward trend that was correlated with a similar trend in the North Atlantic Oscillation (NAO) index. The changing sign of this index can explain a substantial portion of the climatic variability over the Atlantic sector and has an intimate connection with weather patterns in the Arctic Basin [*Serreze et al.*, 2000; *Deser et al.*, 2000; *Vinje*, 2000; *Parkinson*, 2000; *Tucker et al.*, 2001]. During periods of high NAO index, when both the Azores High and Icelandic Low are strong, northerly winds prevail over the Greenland Sea region and favor increased ice export through Fram Strait, such as occurred during the 1980s and 1990s.

[32] Model simulations were used by *Harder et al.* [1998] and by *Arfeuille et al.* [2000] to derive a time series of ice export beginning in 1958. These studies showed that besides the 1990s, large positive anomalies in volume export also occurred in 1959, 1967–1968, 1981–1982, and 1989. *Arfeuille et al.* [2000] argue that a number of these earlier export anomalies were due to the presence of very thick ice in the basin, whereas the large volume export in the 1990s was mainly due to strong northerly winds in Fram Strait which produced increased area flux. This conclusion is supported by their discovery that large ice export events in the earlier years lagged volume anomalies in the basin by about two years.

[33] Under steady state conditions net ice production in the basin is balanced by ice export, primarily through Fram Strait. When changes in thermal forcing or ice advection occur, however, this balance may be upset and act to shift the system toward a new steady state condition. Although exact steady state is unlikely to ever be achieved owing to constantly shifting forcing, the idea of a balance between export and net ice production is useful in understanding how the overall system works. Ice exported through Fram Strait causes areas of open water to be created within the basin, the total area created being about the same as the area of ice lost. Subsequent ice growth, rafting, and ridging in these areas are important factors in the development and maintenance of $g(h)$. An increase in the rate of area export produces a corresponding increase in the area of open water created and a decrease in average ice thickness within the basin. On the other hand, ice volume export anomalies caused by changes in $g(h)$ do little to alter the amount of open water formation or the export/ice production balance

within the basin and hence should not have a major impact on average ice thickness. For this reason ice area flux anomalies observed during the late 1980s and 1990s are likely to have had a much larger effect on average ice thickness than the volume flux anomalies observed during the 1960s and 1970s.

6.3. Changes in Ice Growth and Melting Patterns

[34] While it seems evident that changes in ice export played some role in the thinning, it is not clear whether this export was the primary cause or merely a contributing factor in the observed changes. Some clues, however, can be obtained by looking at changes in the shape of $g(h)$ in Figure 7a. Given sufficient time, the primary peak in $g(h)$ in areas of perennial ice should occur near the thermodynamic equilibrium thickness H_e [*Maykut and Untersteiner*, 1971] because both thicker and thinner ice grow toward H_e (i.e., the location of H_e is largely determined by the thermodynamic forcing). If the thickness distribution of ice exported from a region is representative of that region, there should be little impact on the location of the primary peak, although its magnitude could be altered or a secondary peak introduced. This simple picture, however, is complicated by residence time of the ice, spatial and interannual variations in thermal forcing, and by advection of ice between different regions.

[35] These uncertainties can be reduced somewhat by averaging the data over the entire central Arctic and over several different years, as was done in Figure 7; here the fall peak at 1.5 m in $g(h)$ decreased by about 10% between the two periods. It might be argued that this could be explained by more rapid advection of ice associated with greater area export, which would reduce the residence time of the ice, allowing less ice to approach H_e. However, analysis of buoy data by *Rigor et al.* [2002] indicates that changes in residence time were quite small throughout most of the basin. In addition, some of the largest changes in ice thickness occurred in the Canada Basin sector (see Figure 6), the region least affected by variations in ice export through Fram Strait. It thus appears that the decrease in amount of 1.5-m ice was not caused by ice export alone and that reduced ice growth and/or increased summer melting played an important role, suggesting that significant changes in thermal forcing have occurred in the central Arctic.

[36] A variety of different indicators point to changes in Arctic atmospheric circulation. One is a shift in the average pressure pattern. As a result, arctic cyclones have become more common and intense since the mid-1960s [*Serreze et al.*, 2000], suggesting increased poleward heat transport by the atmosphere, which may have contributed to rising surface air temperatures observed in many arctic regions. Data from Russian North Pole drifting stations, drifting buoys, and coastal stations show an increased January to July surface air temperature of 0.2°–0.9°C per decade since as early as 1961 [*Serreze et al.*, 2000]. The warming was also evident in the empirical orthogonal functions of surface air temperatures computed by *Wang and Ikeda* [2000]. They showed that there have been several major warming events since the 1970s, the warming in the 1990s being the strongest and longest. All these warming events lasted for at least 4 years and were persistent throughout all four seasons.

[37] An increase in near surface air temperatures would presumably have a direct impact on sea ice thickness. In fact, observations at the North Pole Environmental Observatory in spring 2002 revealed a winter ocean mixed layer that was more shallow and less saline than usual, a sign of a possible decrease in winter ice production (M. Steele, personal communication, 2002). Although increased air temperatures would affect ice growth in all thickness categories, long-term effects will be seen most strongly in the amount of thicker ice. This is due to differences between summer and winter growth rates and to the transformation of thicker ice into thinner. While summer melting of undeformed ice is nearly independent of thickness, winter ice growth rates depend inversely on thickness. This means that during the winter, thinner ice can recover much more of any increased summer mass loss than can thick ice. The result is a progressive loss of thicker ice as has been shown in model simulations by *Bitz and Roe* [2004]. This effect would be magnified by a lengthened melting season. According to passive microwave data collected from 1979 to 1996 by the SMMR and SSM/I satellite sensors, the number of melt days per summer has increased by 5.3 days (8%) per decade [*Smith*, 1998].

[38] Another important consequence of the overall thinning is a positive feedback process that acts to enhance bottom melting, particularly in areas of deformed ice. A substantial amount of the solar radiation absorbed by thinner ice and melt ponds is transmitted through the ice cover and absorbed in the ocean mixed layer. This absorbed heat is subsequently returned to the underside of the ice in the form of an oceanic heat flux that causes bottom melting during the summer or retards ice growth later in the fall. All other things being equal, solar heat transmission to the mixed layer should increase exponentially with decreasing ice thickness, leading to further heating and additional thinning, a classic positive feedback that acts to magnify the effect of changes in climate on average ice thickness. Model simulations [e.g., *Maykut and Untersteiner*, 1971] indicate that H_e is very sensitive to even small changes in the oceanic heat flux and the amount of bottom melting.

[39] Because of increased turbulence and greater surface area, pressure ridge keels tend to receive more of this oceanic heat and to experience greater melting than the surrounding flat ice. The effects of this process were evident during the Surface Heat Budget of the Arctic Ocean (SHEBA) 1998 experiment where multiyear ice floes, and especially deformed ice, were observed to experience greater thickness losses than the smoother first-year floes. The large mass losses at the bottom were almost certainly related to the relative thinness (<2 m) of the ice that allowed enhanced transmission of solar radiation to the ocean in the vicinity of the SHEBA station. While most of this heat contributed directly to bottom ablation, observations by *Macdonald et al.* [2002] indicate that some could be sequestered and released slowly over extended periods of time. Using the stable isotopic ($\delta^{18}O$) composition of sea water collected during the SHEBA drift, they found an exceptional high inventory of fresh water, elevated by ice melt but primarily by the Mackenzie River runoff, penetrating to a depth of 20–30 m where sensible heat was

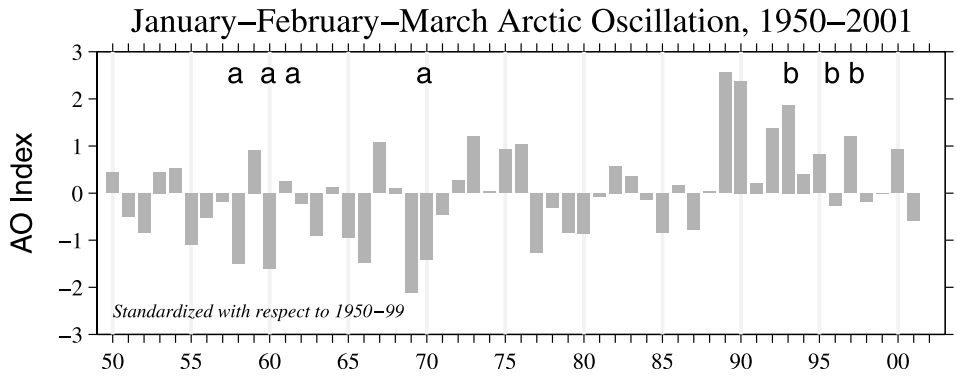

Figure 11. Winter (December through March) AO index, based on the difference of normalized sea level pressures between Lisbon, Portugal, and Stykkisholmur, Iceland, from 1984 to 2000. The index was negative during most of the early cruise years (indicated by the letter "a") and positive during the later cruises (indicated by the letter "b").

trapped by the increased stratification. Release of this heat later in the year would have a much greater impact on thicker ice than on thin ice; during the early fall, for example, a small oceanic heat flux could allow the ablation of thicker ice to continue and, at the same time, allow thin ice to grow rapidly. In any case, the model results and SHEBA data indicate that solar heating of the oceanic mixed layer is likely to have been a major factor in shifting the peak of $g(h)$ (Figure 7a) and in reducing the proportion of thicker ice.

6.4. Changes in Ice Deformation

[40] The SCICEX data have revealed large losses in the amount of thicker ice, particularly in the proportion of very thick, ridged ice that has become increasingly rare. Basin-wide, ice thicker than 8 m accounted for about 9% of the area in the 1960s and only about 2% in the 1990s; less than 1% of the ice was thicker than 10 m in the 1990s. As noted above, both ice export and warming act to reduce the amount of thicker ice, but other factors could also contribute to the reduction. Increased ice area export, for example, is likely to produce greater divergence and reduced ridging rates within the central basin. It is also possible that thinner floes may not be able to support the deep rubble piles associated with the formation of very thick ridges, making it more difficult for them to be created.

[41] While there are no direct measurements to show that the rate of ice ridging has decreased in recent years, some evidence does indicate a shift in the ice motion fields that could be connected to decreased ice ridging. An analysis of drift data from the arctic buoy array shows a correlation between decadal variations in ice motion and the high/low phases of the Arctic Oscillation (AO) [*Rigor et al.*, 2002]. According to this study, the Beaufort Gyre was much stronger during periods of low AO index. Strong cyclonic circulation pushed ice from the western Arctic into the East Siberian Sea, weakening direct advection of ice from the East Siberian and Laptev Seas via the Transpolar Drift Stream and causing ice to circulate longer within the Arctic Basin. When the index was high, however, both winter and summer ice motion fields were highly correlated with the AO index and area flux from the west to the east almost vanished. There was also about a 10% increase in area flux through Fram Strait and a doubling of divergence rates in the eastern Arctic; ice divergence for the entire basin increased by about 13%. The winter AO index (January–February–March) was generally negative for 1950–1988 and positive for 1989-present (Figure 11). The persistent negative phase of the AO coincides with the period of thicker and more ridged ice during 1958–1970, and the positive phase with the thinner ice observed during the SCICEX cruises. Because of the increased divergence the positive phase is likely to weaken ridging and lead to a less compacted ice cover that favors the growth of young ice and the rapid flushing of ice from the basin. The correlation between the AO index and time-dependent differences in $g(h)$ suggests that a significant part of the observed changes in the ice cover are part of some longer-term cycle that could recover when the AO shifts back to a negative phase.

7. Summary

[42] A previous analysis of submarine observations [*Rothrock al.*, 1999] indicates that mean ice draft at the end of the melt season decreased throughout most of the deep water portions of the Arctic Basin over the past several decades, from about 3.1 m in 1958–1970 to 1.8 m in 1993–1997. In this paper, we expand the earlier study to examine differences in the ice thickness distribution between the two periods, using an augmented set of submarine data from some of the same cruises. Comparisons of ice draft measurements between the two periods show that the fractional coverage of first-year ice ($h < 1$ m) increased from less than 20% of the area in 1958–1970 to almost one third of it in 1993–1997. While the coverage of 1–2 m ice increased from 24% to 33%, there was a decrease in all thicker ice categories. The overall volume loss was about 32%, which is 8% less than the value reported by *Rothrock et al.* [1999]. The main cause of this difference is that more submarine tracks are included in this analysis, in particular those in the Chukchi Sea. Because the cumulative volume of ice thinner than 4 m was nearly the same during the two periods, the net loss in volume was caused almost entirely by a large reduction in the amount of ridged ice.

[43] The exact reasons for the observed changes in $g(h)$ cannot be established with certainty from the available data,

but both increased area export through Fram Strait and general warming are likely to have been involved. Surprisingly, the increased ice export and greater divergence within the basin seem to have had relatively little impact on the thickness distribution and volume of ice in the eastern Arctic (Figures 6 and 9), the location of which is slightly different from that defined by *Rothrock et al.* [1999]. Buoy data, however, indicate that the Beaufort Gyre shifted westward during the 1990s so that the central Arctic sector (as defined here) was entirely within the Transpolar Drift Stream [*Rigor et al.*, 2002]. The dramatic increase in thinner ice seen there (Figure 6) suggests that the amount of thin ice and open water in the vicinity of the North Pole may have a more direct link to the export rate through Fram Strait than to regions further upstream. We do not believe this to be the case in the Canada Basin sector, which was within the Beaufort Gyre during both periods and which should be only weakly affected by export variations. Changes in this sector were comparable to those in the central Arctic but were presumably driven mostly by warming air temperatures, a prolonged melt season, and strong feedback between thinning ice and solar heating of the upper ocean. While these same factors would also have contributed to thinning in the central Arctic, their relative importance is difficult to determine because of changes in the location of the Transpolar Drift Stream. Nevertheless, the evidence indicates that increased thermal forcing has reduced H_e and played a major role in changing the overall position of the peak in $g(h)$ (Figure 7). This brings into question the hypothesis of *Holloway and Sou* [2002] that changes in average ice thickness are due primarily to the advection and ''pileup'' of ice along the coastal regions of the Canadian Archipelago.

[44] Decadal variations of the NAO and AO indexes correlate with the interannual variability of the ice thickness distribution observed between 1958–1970 and 1993–1997, as well as with ice export anomalies in Fram Strait. At the same time, changes in the shape of $g(h)$ and other field data suggest changes in thermal forcing. Unfortunately, the ice thickness record by itself does not provide sufficient information to establish the relative importance of changes in dynamic and thermodynamic forcing. Yet this is important because changes due to variations in ice export can potentially be reversed, even if climate continues to warm. Large-scale model simulations offer the best way to obtain a more quantitative picture of the degree to which climate change has affected overall ice thickness.

[45] **Acknowledgments.** We thank the U.S. Navy for the extraordinary opportunity presented by the SCICEX program and to the staff of the Arctic Submarine Laboratory for their expertise in SCICEX cruise planning and data preprocessing. We are grateful to Mark Wensnahan, who provided the digitized analog profile data. We also gratefully acknowledge A. Thorndike and N. Untersteiner for providing many helpful suggestions on the manuscript. Comments by R. Kwok, C. Parkinson, and R. Macdonald were very helpful in improving the paper. This work was supported by the National Science Foundation through grants OPP-9617343, OPP-0084271, and OPP- 9910331, and by a joint ONR-NASA grant NAGW-5177.

References

Arfeuille, G., L. A. Mysak, and L. B. Tremblay (2000), Simulation of the interannual variability of the wind-driven Arctic sea-ice cover during 1958–1998, *Clim. Dyn.*, *16*, 107–121.

Bitz, C. M., and G. H. Roe (2004), A physical explanation for the high rate of sea-ice thinning in the Arctic Ocean, *J. Clim.*, in press.

Bourke, R. H., and A. S. McLaren (1992), Contour mapping of Arctic Basin ice draft and roughness parameters, *J. Geophys. Res.*, *97*, 17,715–17,728.

Carmack, E. C., R. W. Macdonald, R. G. Perkin, F. A. Mclaughlin, and R. Pearson (1995), Evidence for warming of Atlantic water in the southern Canadian Basin of the Arctic Ocean: Results from the Larsen-93 Expedition, *Geophys. Res. Lett.*, *22*, 1061–1064.

Deser, C., J. E. Walsh, and M. S. Timlin (2000), Arctic sea ice variability in the context of recent atmospheric circulation trends, *J. Clim.*, *14*, 255–267.

Gloersen, P., and W. J. Campbell (1991), Recent variations in Arctic and Antarctic sea-ice covers, *Nature*, *352*, 33–36.

Harder, M., P. Lemke, and M. Hilmer (1998), Simulation of sea ice transport through Fram Strait: Natural variability and sensitivity to forcing, *J. Geophys. Res.*, *103*, 5595–5606.

Holloway, G., and T. Sou (2002), Has arctic sea ice rapidly thinned?, *J. Clim.*, *15*, 1691–1701.

Johannessen, O. M., E. V. Shalina, and M. Miles (1999), Satellite evidence for an Arctic sea ice cover in transformation, *Science*, *286*, 1937–1939.

Kwok, R., and D. A. Rothrock (1999), Variability of Fram Strait ice flux and North Atlantic Oscillation, *J. Geophys. Res.*, *104*, 5177–5189.

LeSchack, L. A. (1980), Arctic Ocean sea-ice statistics derived from the upward-looking sonar data recorded during five nuclear submarine cruises, *ONR Tech. Rep. N00014–76–C-0757/NR 307–374*, 15 pp., LeSchack Assoc., Silver Spring, Md.

Macdonald, R. W., F. A. McLaughlin, and E. C. Carmack (2002), Fresh water and its sources during the SHEBA drift in the Canada Basin of the Arctic Ocean, *Deep Sea Res.*, *49*, 1769–1785.

Martin, S., E. Munoz, and R. Dreucker (1997), Recent observations of a spring-summer warming over the Arctic Ocean, *Geophys. Res. Lett.*, *24*, 1259–1262.

Maslanik, J. A., and J. Dunn (1997), On the role of sea-ice transport in modifying Arctic responses to global climate change, *Ann. Glaciol.*, *25*, 102–106.

Maykut, G. A. (1982), Large-scale heat exchange and ice production in the central Arctic, *J. Geophys. Res.*, *87*, 7971–7984.

Maykut, G. A., and M. G. McPhee (1995), Solar heating of the Arctic mixed layer, *J. Geophys. Res.*, *100*, 24,691–24,703.

Maykut, G. A., and N. Untersteiner (1971), Some results from a time-dependent thermodynamic model of sea ice, *J. Geophys. Res.*, *76*, 1550–1575.

McLaren, A. S. (1989), The under-ice thickness distribution of the Arctic Basin as recorded in 1958 and 1970, *J. Geophys. Res.*, *94*, 4971–4983.

McPhee, M. G., T. P. Stanton, J. H. Morison, and D. G. Martinson (1998), Freshening of the upper ocean in the Arctic: Is perennial sea ice disappearing?, *Geophys. Res. Lett.*, *25*, 1729–1732.

Morison, J., M. Steele, and R. Anderson (1998), Hydrography of the upper Arctic Ocean measured from the nuclear submarine, USS *Pargo*, *Deep Sea Res.*, *45*, 15–38.

Parkinson, C. L. (2000), Recent trend reversals in Arctic sea ice extents: Possible connections to the North Atlantic Oscillation, *Polar Geogr.*, *24*, 1–12.

Parkinson, C. L., and D. J. Cavalieri (2002), A 21 year record of Arctic sea-ice extents and their regional, seasonal and monthly variability and trends, *Ann. Glaciol.*, *34*, 441–446.

Parkinson, C. L., D. J. Cavalieri, P. Gloersen, H. J. Zwally, and J. C. Comiso (1999), Arctic sea ice extent, area, and trends, *J. Geophys. Res.*, *104*, 20,837–20,856.

Perovich, D. K., T. G. Grenfell, J. A. Richter-Menge, B. Light, W. B. Tucker, and H. Eicken (2003), Thin and thinner: Sea ice mass balance measurements during SHEBA, *J. Geophys. Res.*, *108*(C3), 8050, doi:10.1029/2001JC001079.

Polyakov, I. V., and M. A. Johnson (2000), Arctic decadal and interdecadal variability, *Geophys. Res. Lett.*, *27*, 4097–4100.

Proshutinsky, A. Y., and M. A. Johnson (1997), Two circulation regimes of the wind-driven Arctic Ocean, *J. Geophys. Res.*, *102*, 12,493–12,514.

Quadfasel, D. (1991), Warming in the Arctic, *Nature*, *350*, 385.

Rigor, I. G., J. M. Wallace, and R. L. Colony (2002), On the response of sea ice to the Arctic Oscillation, *J. Clim.*, *15*, 2648–2663.

Rothrock, D. A., Y. Yu, and G. A. Maykut (1999), Thinning of the Arctic sea-ice cover, *Geophys. Res. Lett.*, *26*, 3469–3472.

Serreze, M. C., J. E. Walsh, F. S. Chapin III, T. Osterkamp, M. Dyurgerov, V. Romanovsky, W. C. Oechel, J. Morison, T. Zhang, and R. G. Barry (2000), Observational evidence of recent change in the northern high-latitude environment, *Clim. Change*, *46*, 159–207.

Smith, D. M. (1998), Recent increase in the length of the melt season of perennial Arctic sea ice, *Geophys. Res. Lett.*, *25*, 655–658.

Steele, M., and T. Boyd (1998), Retreat of the cold halocline layer in the Arctic Ocean, *J. Geophys. Res.*, *103*, 10,419–10,435.

Thorndike, A. S., D. A. Rothrock, G. A. Maykut, and R. Colony (1975), The thickness distribution of sea ice, *J. Geophys. Res.*, *80*, 4501–4513.
Tucker, W. B., III, and W. D. Hibler III (1986), Variability of Arctic sea ice drafts, paper presented at Ice Penetration Technology Workshop, Monterey, Calif.
Tucker, W. B., III, J. W. Weatherly, D. T. Eppler, D. Farmer, and D. Bentley (2001), Evidence for the rapid thinning of sea ice in the western Arctic Ocean at the end of the 1980s, *Geophys. Res. Lett.*, *28*, 2851–2854.
Vinje, T. (2000), Anomalies and trends of sea-ice extent and atmospheric circulation in the Nordic Seas during the period 1864–1998, *J. Clim.*, *14*, 255–267.
Vinje, T., N. Nordlund, and A. Kvambekk (1998), Monitoring ice thickness in Fram Strait, *J. Geophys. Res.*, *103*, 10,437–10,449.
Wadhams, P., and N. R. Davis (2000), Further evidence of ice thinning in the Arctic Ocean, *Geophys. Res. Lett.*, *27*, 3973–3975.
Walsh, J. E., and W. L. Chapman (2001), 20th-century sea-ice variations from observational data, *Ann. Glaciol.*, *33*, 444–448.
Walsh, J. E., W. L. Chapman, and T. L. Shy (1996), Recent decrease of sea level pressure in the central Arctic, *J. Clim.*, *9*, 480–486.
Wang, J., and M. Ikeda (2000), Arctic oscillation and Arctic sea-ice oscillation, *Geophys. Res. Lett.*, *27*, 1287–1290.
Zhang, J., R. A. Rothrock, and M. Steele (2000), Recent changes in Arctic sea ice: The interplay between ice dynamics and thermodynamics, *J. Clim.*, *13*, 3099–3114.

G. A. Maykut, D. A. Rothrock, and Y. Yu, Polar Science Center, Applied Physics Laboratory, University of Washington, Seattle, WA 98105, USA. (yanling@apl.washington.edu)